Distribution of holmium-166 acetylacetonate microspheres after intratumoral injection in a rabbit VX-2 tumour model. A pilot study.

Faculty of Veterinary Medicine, Utrecht, The Netherlands
drs. Bo Sybren van Leeuwen
December 2011 - February 2012

Supervisors:
Prof. dr. J. Kirpensteijn
Dr. J.F.W. Nijsen
Dr. S.A. van Nimwegen

Image front cover: VX-2 tumour bearing Rabbit inside a Single Photon Emission Computed Tomography (SPECT) scanner.

This research project has been conducted in order to meet the requirements for the course 'research stage, curriculum 2001' at the Faculty of Veterinary Medicine, Utrecht, The Netherlands.

Inhoudsopgave

Distribution of ^{166}HoAcAcMS after intratumoral injection in VX-2 tumour bearing rabbits. A pilot study.

Abstract

In order to optimize and standardize ^{166}HoAcAcMS microbrachy therapy, more insight is needed in the distribution of ^{166}HoAcAcMS after intratumoral injection. For that reason, a pilot was conducted to investigate the distribution patterns of the ^{166}HoAcAcMS after intratumoral injection in VX-2 Tumour bearing rabbits and the feasibility of using *in vivo* Multimodality imaging for this purpose. 3 NZW rabbits were used for this purpose and supplied with a VX-2 tumour on both hindpaws yielding 4 usable tumours. The animals were randomly assigned to receive either 1,3 or 6 injections intratumorally. The amount of injected activity and corresponding weight in ^{166}HoAcAcMS varied between 10.5-36.3 (MBq) and 1.56-5.40 (mg) respectively. Multimodal imaging (MRI, CT, SPECT) was performed on day -2, 0, 5 and 9. Qualitative visual analysis revealed a heterogeneous HoAcAcMS distribution in all tumours. Also HoAcAcMS patterns could be recognised and included, string and funnel like formations, dense depots, and interconnected HoAcAcMS filled pathways. No substantial visual pattern change in HoAcAcMS was observed between the MRI images of day 0,5 and 9. Finally, the HoAcAcMS tumour coverage for 1, 3, 6 injection sites shortly after treatment (day 0) was calculated to be 33.9%, 57.4%, 11.6% respectively. In conclusion, multimodality imaging for the purpose of investigating *in vivo* distribution of ^{166}HoAcAcMS after intratumoral injection is feasible and optimising the scan protocols for a larger experimental set-up should be a priority.

Introduction

At the Faculty of Veterinary Medicine Utrecht an experimental cancer treatment is being investigated in close collaboration with the University Medical Center Utrecht (UMCU). In short, this treatment named interstitial microbrachytherapy, entails intratumoral injection of microspheres (approximately 15 µm) loaded with radioactive holmium-166 acetylacetonate (^{166}HoAcAcMS). Holmium-166 emits high energetic beta particles with a tissue penetration of 8,6 mm at maximum and has a short half-life (26.8 h). Holmium-166 also emits low energy gamma radiation traceable using nuclear imaging like single-photon emission computed tomography (SPECT). Furthermore, it shows paramagnetic properties and has a high linear attenuation coefficient making imaging with magnetic resonance imaging (MRI) and computed tomography (CT) possible (1, 2).

By directly injecting radioactive holmium microspheres within the tumour, healthy surrounding tissue is to remain intact while the cancerous tissue receives a large dose of ionizing radiation that has the potential to reduce or even lead to complete tumour ablation. This treatment could be an outcome for human and veterinary patients with solid malignant tumours that can't be treated with surgery, radiation therapy and chemotherapy. Previous research investigating the feasibility of interstitial microbrachytherapy using ^{166}HoAcAcMS for the treatment of intrahepatic malignancies in cats showed promising results (3).

In order to optimize and standardize this promising treatment, more insight is needed in the distribution of ^{166}HoAcAcMS after intratumoral injection. Previous attempts to investigate the distribution of ^{166}HoAcAc-MS in agar phantoms and *ex vivo* tissue samples (e.g. dog brains and chicken breast) showed disappointing results and are poor models for *in vivo* tumours (4, 5). Therefore, experiments have to be performed on *in vi*vo tumour tissue. Preferably of the same tumour type and on similar tumour bearing animals. Doing so, the results can be compared and the possible change in distribution over time can be closely studied using multimodality imaging (MRI, SPECT and CT).

In the presented pilot study we aim to investigate the distribution patterns of the ^{166}HoAcAcMS after intratumoral injection(s) in a VX-2 tumour model. Because it is thought that a better dose distribution is accomplished with more intratumoral injections in larger growing tumours, all tumours will receive either one, three or six intratumoral injections at random (6, 7). Different *in vivo* multimodality imaging (MRI, CT, SPECT) will be used to investigate the distribution pattern of ^{166}HoAcAcMS. Also the feasibility using these modality's for this purpose will be evaluated. Furthermore, possible changes in this distribution pattern will be monitored over a 9 day time period after ^{166}HoAcAcMS injection.

Material and Methods

Animal model

Three female New Zealand White River rabbits, approx. 12-15 months old and weighing 3.0-3.5 kg were acquired from Charles River Laboratories . Prior to the experiments, a two week acclimatisation period was respected. Before ^{166}Ho-AcAc-MS treatment, the animals were held in groups (2 rabbits per cage), after treatment they were kept individually under the same standard laboratory conditions (Gemeenschappelijk Dier Laboratorium, Utrecht). All animals were supplied pellets 100 gram p/day, quality hay and water ad libitum. Cage enrichment was supplied in the form of a bite ball filled with quality hay. All animal experiments were approved by the animal experimental committee, Utrecht, the Netherlands (DEC no: 2011.III.08.080) and were conducted in agreement with the Netherlands Experiments on Animals Act and the European convention guidelines.

Tumour growth

The VX-2 cell line used for growing the VX-2 tumour used for transplantation was originally supplied by d. R.J.J. van Es (8). The VX-2 tumour used for transplantation was derived from a NZW rabbit from a different study already bearing the VX-2 tumour, given by drs. J. Wijlemans. Viable tumour pieces were obtained by using a non-necrotic part of the aseptically prepared and excised VX-2 tumour (as described earlier (9)). Immediately thereafter, obtained pieces were cut in small portions of approx. 1 mm^3 and submerged in ice-cold PBS solution.

Tumour growth was achieved by subcutaneously injecting three viable VX-2 tumour pieces (approx. 1mm^3) on both upper hind legs using a 18 G abbocoth needle. The tumours were allowed to grow for 3 weeks and were monitored by using a calliper to measure their dimensions (height, width, length) on a day to day basis.

Anesthesia, analgesia and euthanasia

Sedation during MRI and SPECT/CT imaging was achieved with dexmedetomidine[1] i.m 0,125 mg kg^{-1} , glycopyrrolate[2] s.c. 0.1 mg kg^{-1} and ketamine[3] i.m. 15 mg kg^{-1}. After completing the imaging protocol, atipamezole[4] s.c. was administered at the same volume of dexmedetomidine[1].
Anaesthesia during the ^{166}Ho-AcAc-MS treatment and surgical excision of the tumour was achieved with fentanyl 8 µg/kg i.m. and by inhalation of isoflurane (1.5-4% 0_2/air 1:1) through a facemask.
For post-operative analgesia Meloxican[5] 0.5 mg kg^{-1} s.c was given once.
The animals were euthanized after 9 days post treatment by i.v. injection of pentobarbital[6] 100-200 mg corresponding to 0.5-1 ml respectively at the marginal ear vein.

Holmium acetylacetonate microsphere preparation

Holmium-165 acetylacetonate microspheres (^{165}HoAcAcMS) with a size distribution 10-20 µm (mean 15 µm) and holmium content of 43% (by weight) were prepared using a solvent evaporation process, as previously described (10). 98 mg of ^{165}HoAcAcMS were neutron activated in a nuclear reactor (University of Technology, Delft, The Netherlands) with a thermal neutron flux of $5x10^{12}$ n $cm^{-2}s^{-1}$ for 49 minutes. After neutron irradiation, the holmium microspheres were suspended in sterile water containing 2% PluronicF68 and 10% ethanol abs. by repeatedly drawing it up and down a 18 gauge needle attached to a 1 ml syringe. Subsequently, the suspension was drawn up using a 27 gauge needle attached to a 1 ml syringe until the amount of radioactivity present in each syringe (n=11) was close to the pre-calculated needed activity. The amount of radioactivity in each syringe was measured in a dose calibrator (VDC-404, Veenstra Instruments).

Radioactive Dose calculation

The rabbits were randomly assigned to receive either 1, 3 or 6 ^{166}HoAcAcMS injections intratumorally. One day prior to treatment the tumour dimensions were measured with a calliper to calculate the tumour volume using the formula:

$$V = \frac{4\pi}{3}\left(\frac{L \times W \times H}{8}\right) \quad [cm^3]$$

where

V is the tumour volume [cm^3]
L is the tumour length [cm]
W is the tumour width [cm]
H is the tumour height [cm]

All tumours were intended to receive a total absorbed dose of 200 Gy. The amount of activity needed for each tumour was calculated using the formula (11):

$$A = \frac{200}{15.87} W_t \quad [MBq]$$

where

A is the activity [MBq]

---

[1] DEXDOMITOR (0.5 mg/mL), Jansen PharmaceuticaNV, The Netherlands.
[2] Robinul injectable (0.2mg/ml), Riemser Arzneimittel, AG, Germany
[3] Narketan 10 (100mg/ml) Vétoquinol, France.
[4] Atipam (5 mg/mL) Eurovet Animal Health B.V., The Netherlands.
[5] Metacam (5mg/ml), Boehringer Ingelheim Vetmedica GmbH, Germany
[6] Euthesate (200mg/ml); Aesculaap, Boxtel, The Netherlands,

W_t is the tumour weight [g], tissue density was assumed to be 1.0 g ml^{-1} .

Administration of microspheres

Before injection, each syringe was vigorously shaken and stirred to obtain a homogenous suspension. Location of injection was chosen visually by dividing the tumour in equal parts. While manually fixating the tumour, ^{166}HoAcAcMS were intratumorally injected under slow retraction of the needle. Visually leakage of fluid was removed from the skin with cotton gauze. After injection, one tumour was surgical removed. Thereafter, the amount of residual radioactivity (A_{res}) of all the syringes, needles, operating equipment and gauzes were measured in a dose calibrator (VDC-404, Veenstra Instrumenten B.V. Joure, The Netherlands). The total injected radioactive dose (A_{inj}) was calculated using the formula:

$$A_{inj} = A_{res} - A_i \quad [MBq]$$

where

A_{inj} is the total injected activity, at time of administration [MBq]
A_{res} is the residual activity, at time of administration [MBq]
A_i is the initial activity, at time of administration [MBq]

The final absorbed tumour dose was determined by using the tumour volume used to calculate the required amount of activity using the formula (11):

$$D = 15.87 \frac{A_{inj}}{W_t} \quad [Gy]$$

where

D is the tumour absorbed dose [Gy]
A_{inj} is the total injected activity, at time of administration [MBq]
W_t is the tumour weight [g], tissue density was assumed to be 1.0 g ml^{-1} .

MR Imaging

MR imaging of the tumour bearing rabbits was performed on a clinical 1.5 T MRI Scanner using Sense Flex-S coils (Achieva, Philips Medical Systems, Best, Netherlands) 2 days before treatment to acquire pre-treatment images without ^{166}HoAcAcMS. Thereafter, MRI was repeated shortly after ^{166}HoAcAcMS treatment on day 0, day 5 and day 9 after treatment to evaluate ^{166}HoAcAcMS distribution and to monitor tumour response. Anatomical depiction of the tumour was visualised using a T_2Weighted Turbo Spin Echo scan (T_2w TSE) and spatial distribution of ^{166}HoAcAcMS was investigated using 3D Multi Gradient Echo sequences (UTE). Used parameters are summarised in table 1. All acquired MRI images were qualitatively evaluated using ImageJ (version 1.47).The following steps allowed a more systematic analysis of the ^{166}HoAcAcMS distribution.

Visual inspection of holmium sensitive areas inside the image stacks:

1. In other organs besides the tumour and vicinity (e.g. Lungs, abdomen)
2. In the vicinity of the tumour, outside the tumour margins (extra tumoral)
3. Intratumoral

a. Inspection of recognizable distribution patterns (ea. depots and canals)
b. Inspection of a noticeable change in distribution and patterns of ^{166}HoAcAcMS between day 0, 1, 5 and 9

Tumour volume was calculated using MRIcro (version 1.40) by drawing a region of interest (ROI) following the tumour outlines on the anatomical T_2W TSE images.

^{166}HoAcAcMS tumour coverage shortly after treatment was calculated using a predefined threshold value. To determine the HoAcAcMS threshold, a ROI was drawn following the tumour outlines on the T2W TSE images. The resulting tumour ROI was then transferred to the multi gradient UTE

Table I MR imaging parameters.

Parameters	T_2w TSE	UTE
Matrix	160 x 112	160 x 160
FOV [ap,fh,rl mm]	128 x 34 x 128	128 x 128 x 128
Slice thickness [mm]	2	0,5
Number of slices	17	256
Number of signal averages [NSA]	2	1
TR/TE [ms]	2000/40	9/0.34
Number of Echoes	1	1
Flip [°]	90	20
Scan time [min]	2:50	7:42

images acquired at day -2 which did not contain any ^{166}HoAcAcMS. Thereafter, the maximum threshold was downscaled from maximum intensity to the point that almost no voxels were highlighted. The rendered value was considered the cut-off value to differentiate between tumour tissue that contained ^{166}HoAcAcMS, and tumour tissue that did not contain ^{166}HoAcAcMS. Next, the cut-off value was applied on multi gradient UTE images acquired at day 0 (Fig. 1.) The number of voxels within the tumour that were suspected to contain ^{166}HoAcAcMS were then multiplied by the volume (cm^3) they represented. This resulted in a tumour volume suspected to contain holmium on day 0. Finally, the ^{166}HoAcAcMS tumour coverage after intratumoral injection could be calculated using the formula:

$$HoMS\ tumour\ coverage = \frac{V_{HoMS}}{V_t}$$

Where

$V_{HoAcAcMS}$ is the tumour volume suspected to contain holmium on day 0 [cm^3]
V_t is the total tumour volume [cm^3]

CT and SPECT imaging

CT and SPECT imaging of the tumour bearing rabbits was performed on day 1 using a clinical Symbia T16 SPECT/CT system scanner. CT scan settings were 110kV and 18mAs. Different FOV setting and slice thicknesses were used, respectively between 200 mm^3-650 mm^3 and 5 mm-1,5 mm. All acquired CT and SPECT images were visually evaluated using ImageJ (version 1.47).

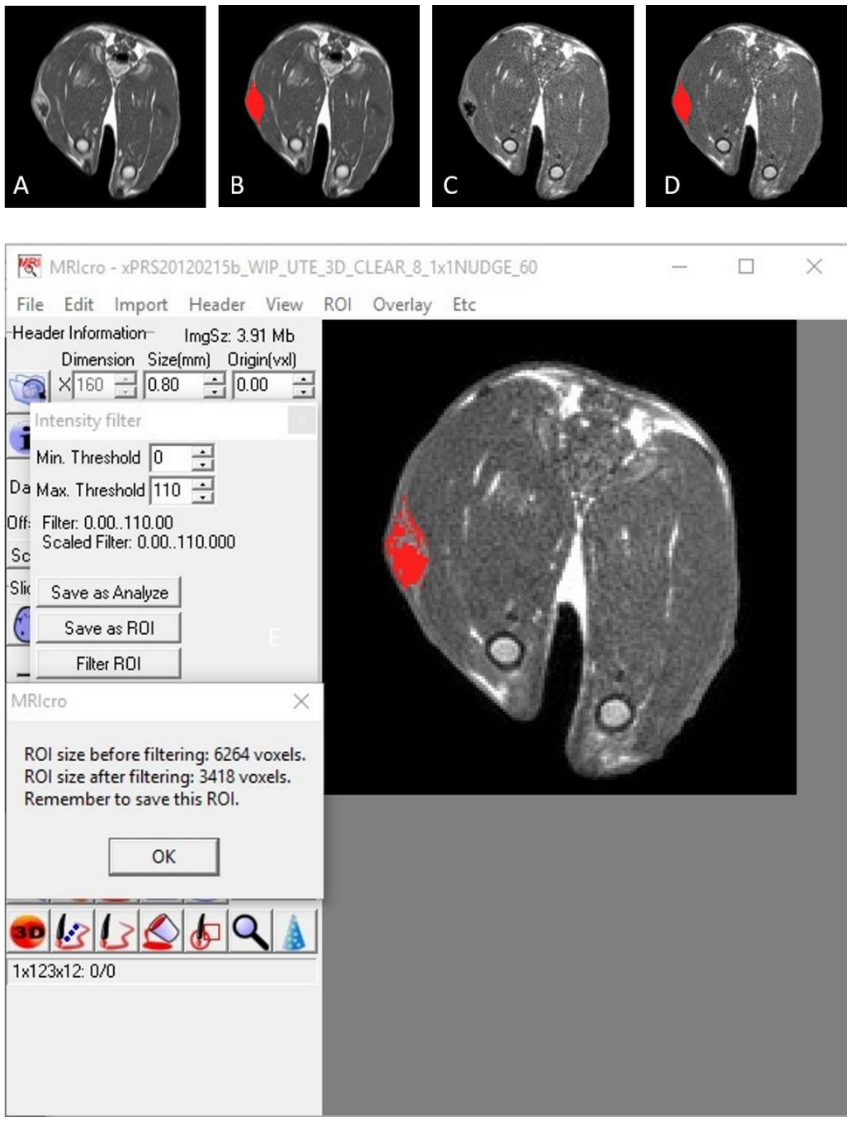

Figure 1. Example of applying the predefined threshold on UTE MRI image stack.

First the tumour is depicted on the T2W TSE image stack (A) and a ROI is drawn using the tumour borders (B). Thereafter, the ROI is transferred to the UTE image stack (C,D) and a intensity filter is applied on the entire ROI volume. This results in a number of susceptible holmium containing voxels (ROI size after filtering, E)

Histology

Tumours were fixated in 3.7 buffered formaldehyde before embedded in paraffin. Subsequently, the tumours were divided into 1.5 mm samples using a cutting board in a sagittal direction (parallel to the skin). From each sample a 4 µm slice was cut and stained using haematoxylin and eosin (H&E). All slices were evaluated for HoAcAcMS presence using light microscopy (12).

Results

Tumour growth and microsphere administration

Tumour growth was accomplished in all three rabbits yielding 4 tumours exceeding 1.0 cm at the time of treatment. Tumour volume was determined at day -1 of treatment by a calliper to determine the required amount of radioactivity. The animals were randomly assigned to receive either 1, 3 or 6 injections intratumorally. The amount of injected activity and corresponding weight in ^{166}HoAcAcMS varied between 10.5-36.3 (MBq) and 1.56-5.40 (mg) respectively (table II). In the tumour that received 6 injections, backflow was noticed from a prior made injection site during the intratumoral injection procedure at a subsequent site. The fluid was removed with cotton gauze and measured for activity in a dose calibrator (Table II).

Tumour volume decreased in 2 rabbits, whereas the 3rd animal tended to show an initial growth before a decrease in size was observed (Table III).

Table II

	Tumour volume* (cm^3)	**Number of injections**	**Initial activity (Mbq)**	**Residual activity (Mbq)**	**Injected dose (MBq)**	**Absorbed dose (Gy)**
Rabbit 1 (136240)	1.7 (L)	1	30.2	3.9	26.2	241.0
	2.2 (R)	1	42.7	5.2 (= 1.5** + 3.7***)	36.3	273.6
Rabbit 2 (136242)	0.7	3	16.6	6.1	10.5	232.8
Rabbit 3 (136330)	2.5	6	46.9	16.3 (= 15.8** + 0.5****)	30.6	195.2

*: calculated using a calliper on day -1
**: all syringes and needles
***: Waste
****: removed fluid from injection site

Table III Tumour volumes calculated using T_2W TSE MR images on day -2, 0, 5 and 9

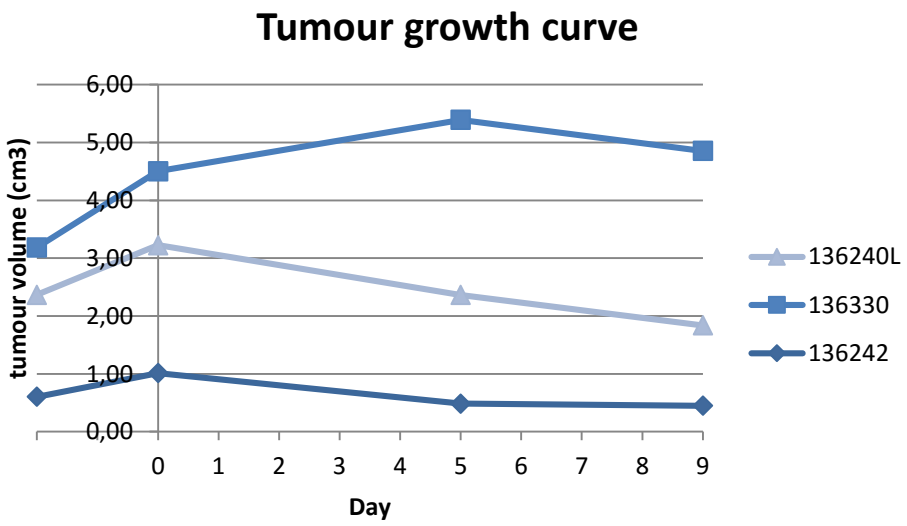

MRI, CT and SPECT analysis

Tumour depiction and HoAcAcMS depositions were clearly visible on the T2W TSE and HoAcAcMS sensitive UTE MR images (fig. 3-5). A heterogeneous HoAcAcMS distribution was observed in all tumours. Inside the tumours, areas were noticed that contained no visible HoAcAcMS. Also, extra HoAcAcMS depostions were seen in extratumoral tissue in the vicinity of the tumour borders. Mostly between the tumour and the skin. HoAcAcMS patterns that could be recognised included, string and funnel like formations, dense depots, and interconnected HoAcAcMS filled pathways (fig. 3-5).

CT images showed a similar pattern seen on MRI, but with less detail (fig. 2A & B). SPECT identified HoAcAcMS activity at tumour locations, but no pattern could be seen due to the low spatial resolution (fig. 2C). A white deposition similar to HoAcAcMS was observed inside the abdomen of one animal on CT. However, SPECT analysis revealed no radioactivity at that specific location.

No substantial pattern change in HoAcAcMS was observed after visual comparison of the MRI images of day 0.5 and 9 (fig. 6-7).

The HoAcAcMS tumour coverage for 1,3,6 injection sites shortly after treatment (day 0) was calculated to be 33.9%, 57.4%, 11.6% respectively.

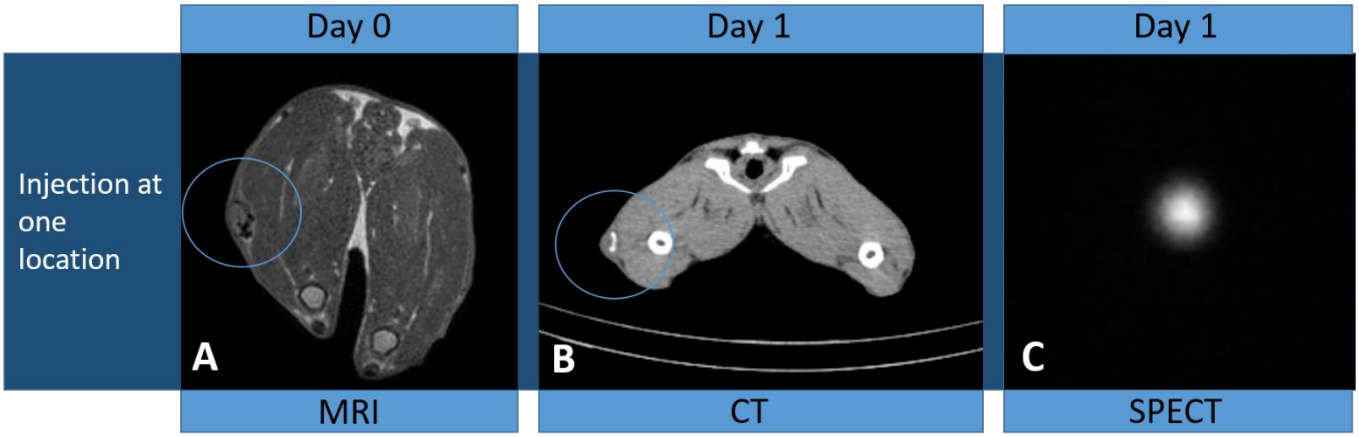

Figure 2. All image modalities used for visualizing HoAcAcMS distribution. Image A shows a transverse HoAcAcMS sensitive UTE (A) slice of the VX-2 tumour injected at one location. Fig B and C show corresponding slices for CT and SPECT respectively. Also, notice the pattern resemblance of MRI and CT (encircled).

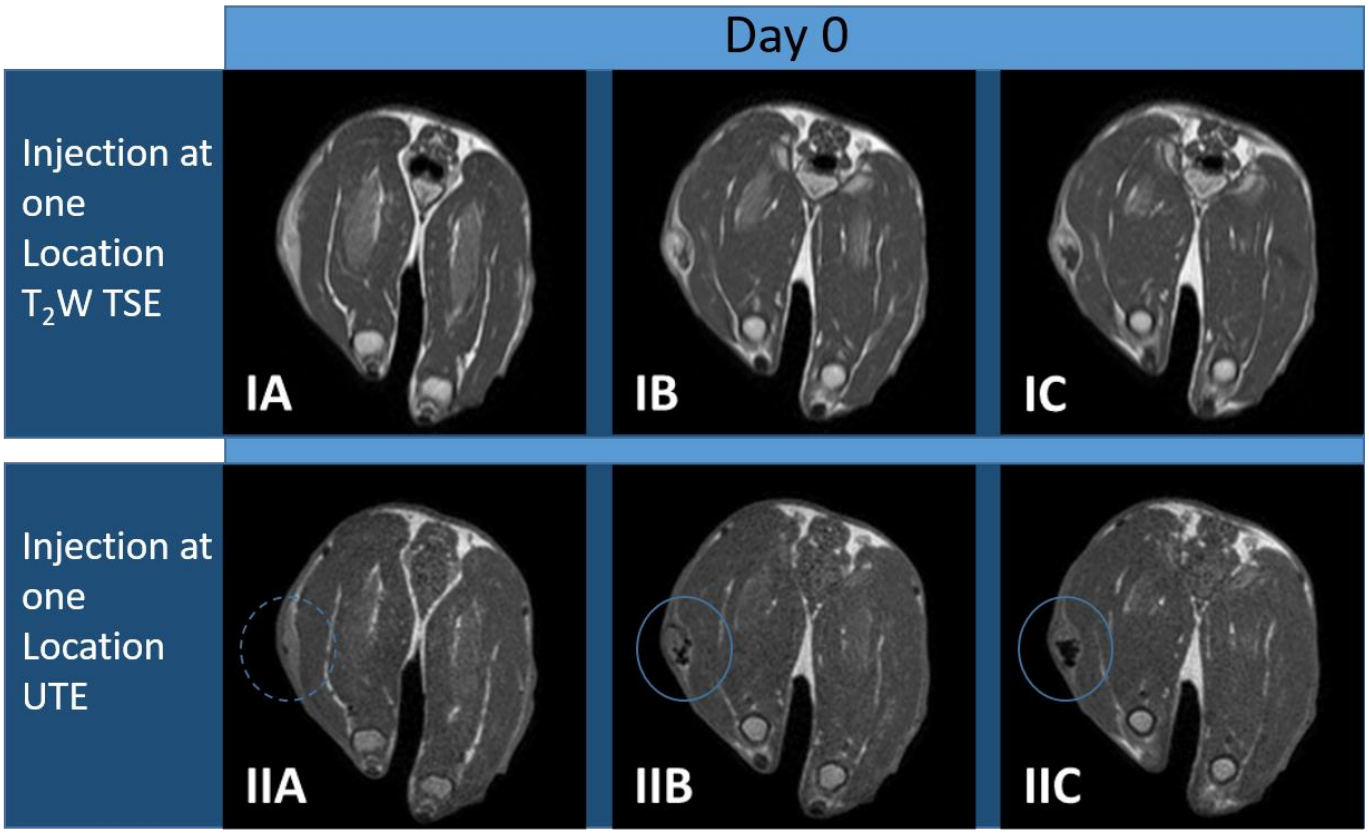

Figure 3. Transverse anatomical T_2W TSE (IA-C) and corresponding HoAcAcMS sensitive UTE (IIA-C) slices of the VX-2 tumour injected at one location. HoAcAcMS are visible as blackening due to dephasing causing signal voids (IIA-C). Images demonstrate tumour tissue lacking HoAcAcMS (IIA), peripheral string like accumulation (IIB) and depots formation of HoAcAcMS (IIC).

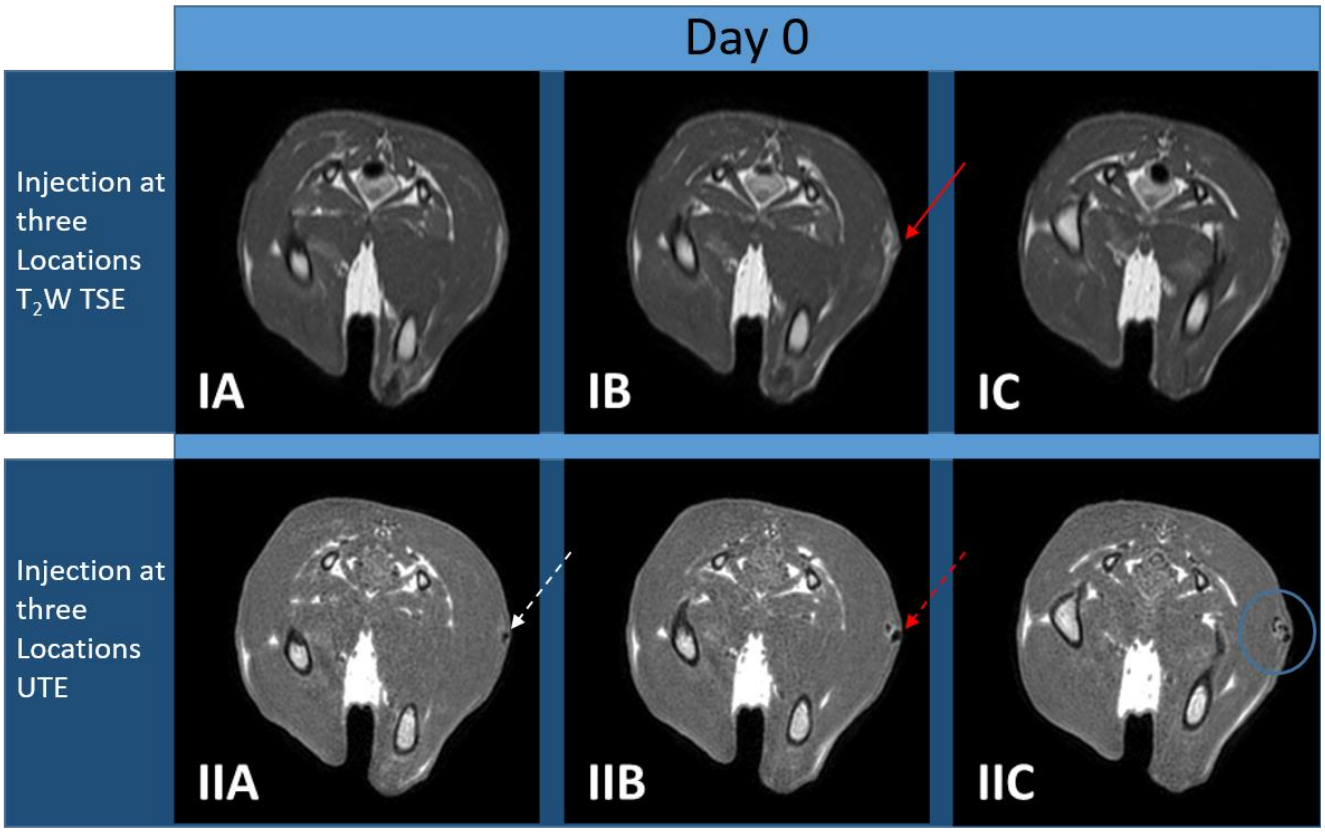

Figure 4. Transverse anatomical T_2W TSE (IA-C) and corresponding HoAcAcMS sensitive UTE (IIA-C) slices of the VX-2 tumour injected at three locations. UTE Slice IIA and IIB shows the presence of extratumoral HoAcAcMS (dotted arrows). Also there is an injection site canal visible on IB (red solid arrow) at the same location as the extra tumoral HoAcAcMS visible on the UTE image (IIB, red dotted arrow).Slice IIC demonstrates a string like HoAcAcMS formation (encircled).

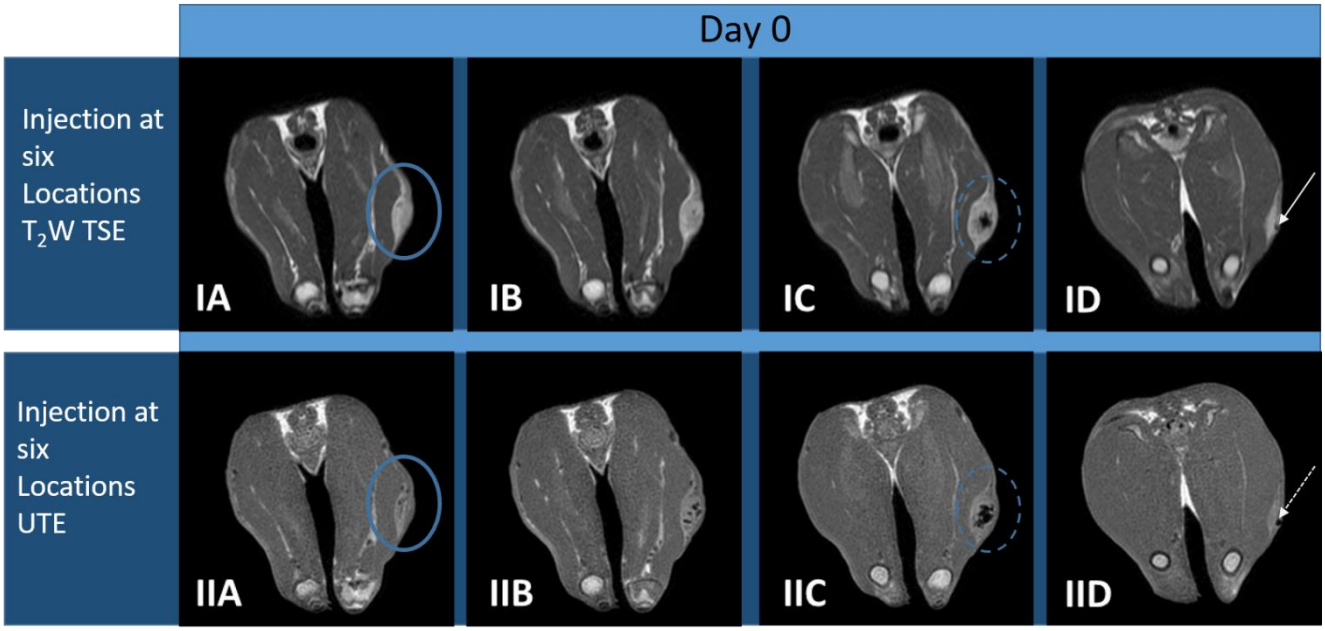

Figure 5. Transverse anatomical T_2W TSE (IA-C) and corresponding HoAcAcMS sensitive UTE (IIA-C) slices of the VX-2 tumour injected at six locations. Images show the lack of HoAcAcMS presence inside tumour tissue (solid circels) and a more centrally located HoAcAcMS depots formation (dotted cirkel). IID shows extratumoral HoAcAcMS (dotted arrow).

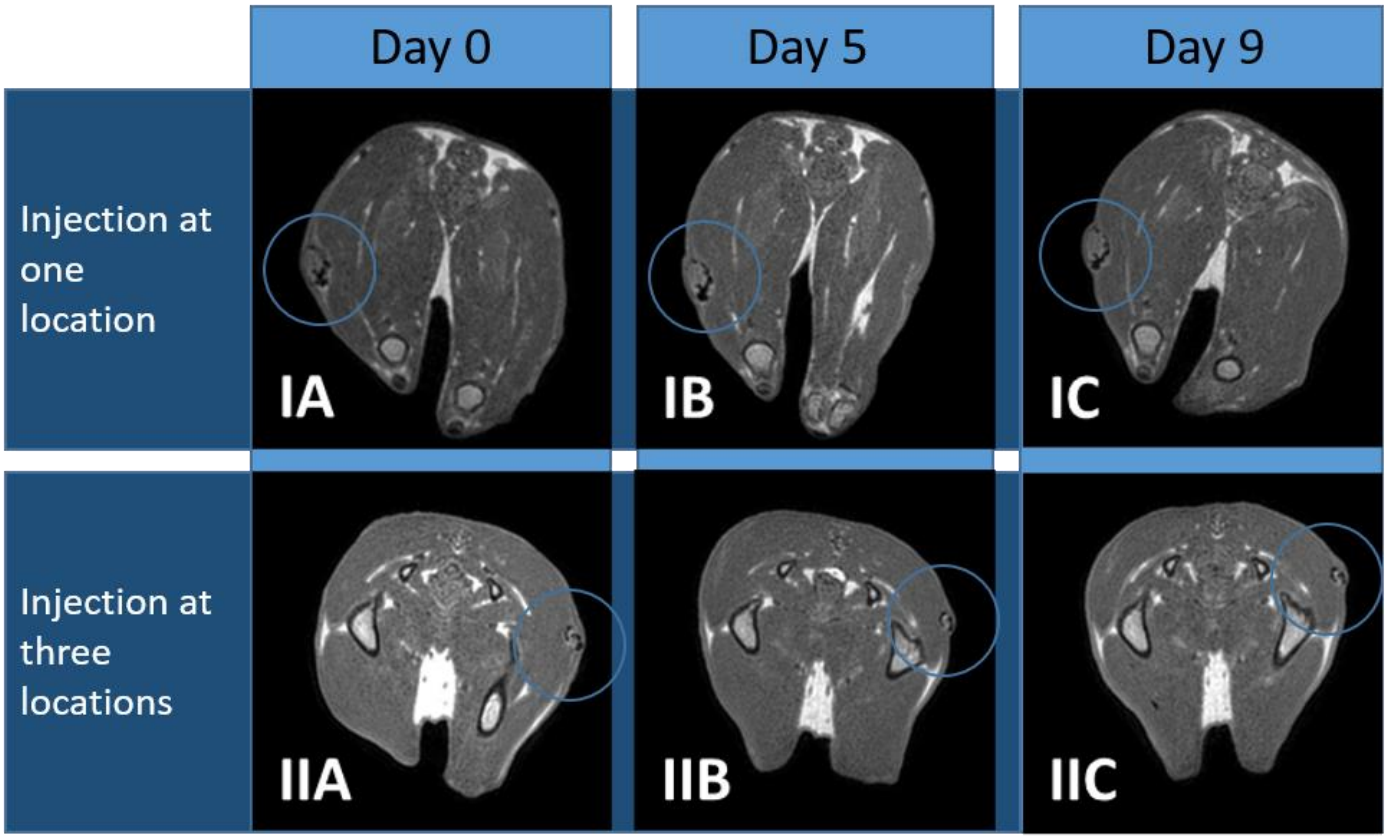

Figure 6. Transverse HoAcAcMS sensitive UTE slices of the VX-2 tumour injected at one (IA-C) and three locations (IIA-C) at day 0 (IA,IIA), 5 (IB,IIB) and 9 (IC,IIC) demonstrating no substantial HoAcAcMS pattern change over time.

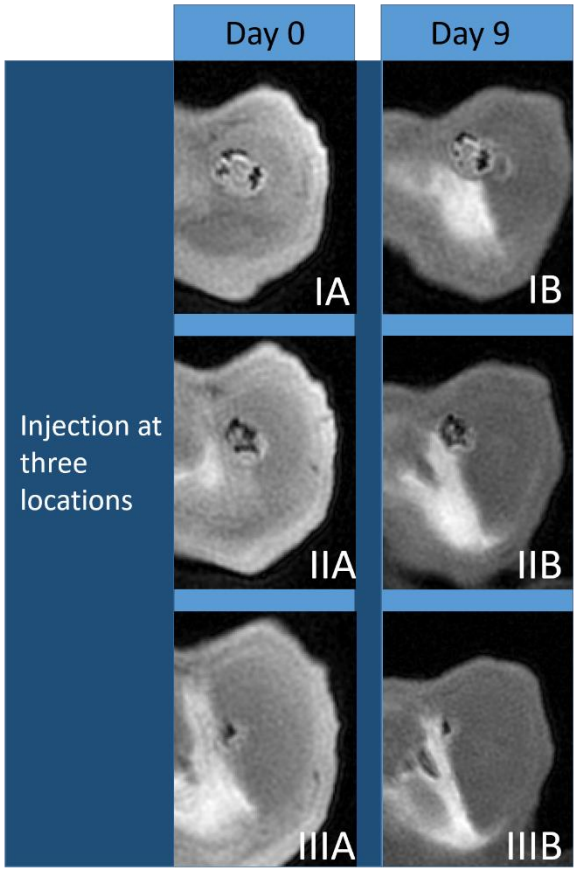

Figure 7. Coronal HoAcAcMS Senstive UTE slices of the VX-2 tumour injected at three locations acquired using a microcoil. The images on Day 0 (IA,IIA,IIA) show no substantial HoAcAcMS pattern change over time compared to the images on day 9

Histology

Histologic evaluation of the tumours showed cluster formation of intact microspheres, mostly surrounded by necrotic tissue (fig. 8). Also areas of continues tumour growth were recognised, devoid of microspheres (12).

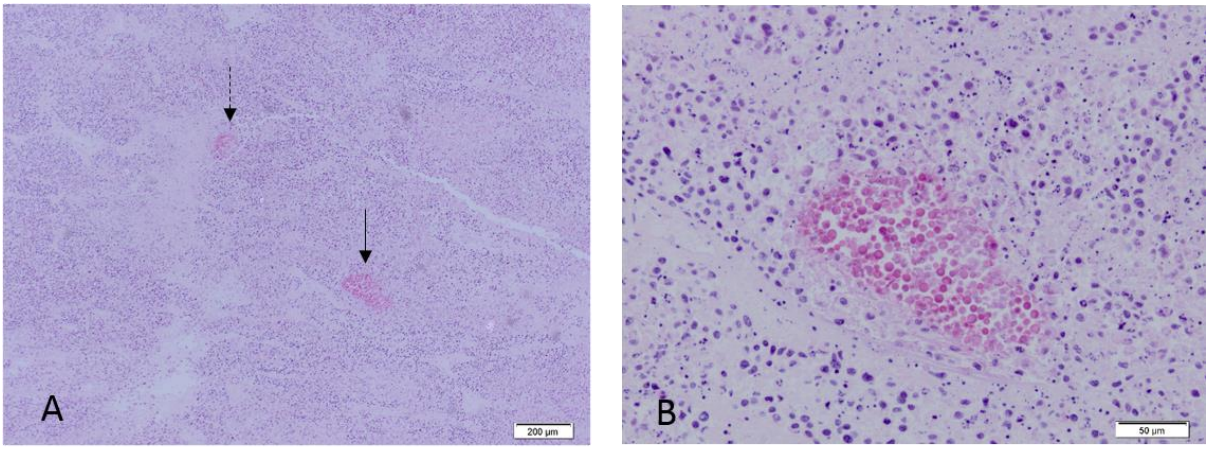

Figure 8. Histologic appearance of the tumour injected at six locations. Plate A shows the purple stained HoAcAcMS cluster formations and surrounding necrotic tissue (arrows, 4x magnification). Plate B shows a close-up under the unbroken arrow of the microsphere cluster (20x magnification).
(Modified from: Brewster SS. Experimental studies on holmium therapy. graduate thesis. Faculty of Veterinary Medicine, Utrecht University: 2012.)

Conclusion & Discussion

In this pilot study, intratumoral injections were given either at one location, three locations or six locations to evaluate difference in distribution pattern in VX-2 tumours over 1.0 cm in diameter. Nakhgevany et al. mentioned in their article that larger tumours need more injections because of the short range of beta emitters like holmium-166 (13). In addition, Bult et al. stated that a tumour larger than 1.0 cm in diameter will benefit from multiple HoAcAcMs injections to facilitate more uniform dose spread (6). Research conducted by Hrycushu et al. reported a more efficient effective uniform dose by using multiple injection sites using computer based distribution models to predict the distribution of infused liposomes encapsulated rhenium radionuclides (7). Interestingly, in our pilot study six injections yielded less tumour coverage than one or three injections (11.6% vs 33.9%, 57.4%, respectively). Findings of interconnected funnel like distribution patterns could be the result of crossing needle paths following intratumoral injection. The initial force driving the HoAcAcMs to spread is most likely caused by the injection force and pressure build up inside the tumour. HoAcAcMs and associated suspension fluid will consequently flow towards the areas with the least resistance. Since different tissue structures have different toughness and permeability, these are important factors to consider while interpreting the pilot results. During the procedure using six injections, backflow of fluid through a prior made injection site was noticed (table II). If the injections crossed each other in close proximity, it seems feasible that the injection fluid and associated HoAcAcMs will spread through already made pathways with low resistance. Thereby causing

backflow through a prior made injection site. Unfortunately, available literature rarely describe the occurrence of backflow through the injection site after intratumoral injection using radiopharmaceuticals. This could be because only one injection is performed in other studies and/or backflow indeed rarely occur or it is not reported when occurring (14). Some efforts to minimize leakage include: final retraction of the needle after the intratumoral pressure returned to normal (15), slow administration over a 10 min period using 10 µl of fluid(16) and mixing the radiopharmaceutical device with fibrin glue to maintain a fixed position after injection(17). Although this pilot group (n=3) is too small to draw definite conclusions about this phenomenon, it must be emphasised that this advert effect must be thoroughly investigated in the near future. Especially when efforts are made in optimizing the technique of microbrachy therapy.

Apart from intratumoral delivery of microspheres, extratumoral depositions of HoAcAcMs were identified on MRI images in close proximity of the tumour rim. A possible cause could be initial extratumoral placement of the injection needle prior to injection of the HoAcAcMs. Also, a needle shaped distribution pattern and associated needle path was identified on UTE and TSE MRI images respectively (fig. 4). These findings suggest filling of the injection needle path with HoAcAcMs that stretched beyond the tumour borders to the skin and underlying subcutaneous structures. To investigate this in more detail in future investigations, histology of the *ex vivo* tumour could be utilized specifically of the areas of interest. Properly placed and carefully documented markers are essential when this approach is used (18). Also more detailed image modalities could be considered, such as micro-CT (1). In future investigations, intratumoral needle placement could be confirmed using ultrasonography to prevent extratumoral depositions of HoAcAcMS. Also, *in vivo* investigation of HoAcAcMS distribution directly after injection using near real-time MRI sequences could be an outcome (19).

HoAcAcMS were not found in other organs besides the tumour tissue and in close proximity of tumours tissue confirmed with MRI, CT and SPECT. A white artefact was seen in the abdomen of one animal but following SPECT, no activity was present at that location. Therefore, the seen artefact on CT was concluded to be of another origin. Other studies regarding intratumoral injection of HoAcAcMs describe microsphere depositions in the lung after treatment. This was attributed to in advert delivery of ^{166}HoAcAcMs in a blood vessel in or around the tumour (6, 20). Although no clear evidence of this phenomenon was observed, it must be emphasised that all image modalities have certain sensitivity and detection limits for HoAcAcMS that must be taken into account (21). Therefore, when more certainty is needed in future research, more sensitive methods should be utilized to investigate this possible adverse distribution to other organs after intratumoral injection of ^{166}HoAcAcMs.

This small pilot study (n=3) shows minimal visual pattern changes in HoAcAcMS depositions over a 9 day time period (fig 6-7). However, Bult et al. described a change in cluster shape formation 4 weeks post intratumoral administration of HoAcAcMs visible on X-ray CT images (20). This could be attributable to a longer interval between injection and evaluation of pattern changes (9 days vs 4 weeks). Also, the position of the animal inside the CT and/or MRI bore and slice orientation of the modality are important factors that can influence the final shape of the object under investigation (e.g. HoAcAcMS cluster shape formations). Small changes in position of the tumour bearing animal inside the bore between scans over time can give the impression of changed HoAcAcMS patterns. Therefore it is important that all investigations are done as consistent as possible. In our study we did not intentionally kept these specific variables consistent. However, it is recommended to write a positioning protocol for the animal inside the imaging modalities for future investigations to increase

comparability between imaging moments. More importantly, visually comparing images and look for considerable change in pattern changes is highly subjective. In our study, one person evaluated all images. It is therefore recommend to revaluate all images by more individuals. Apart from visual inspection, a more quantitative approach would be less subjectable to different interpretations. One suggestion could be Automated calculation of voxel size, curving and roughness of HoAcAcMS patterns by a computer program such as ImageJ. Further work on evaluating pattern changes should focus on designing a standardised model making quantitated comparison possible and give more certain and consist results.

The HoAcAcMs tumour coverage was calculated based on the voxels showing signal voids caused by the paramagnetic HoAcAcMS. It must be emphasized that this method only gives a rough estimate about the total HoAcAcMS coverage inside the tumour tissue as whole. Moreover, it gives no information about the amount of HoAcAcMS (mg) present at any location and as a result no dosimetry could be performed. Since the purpose of holmium brachytherapy is to supply a high radioactive dose to tumour tissue and a minimum dose to the normal surrounding tissue, the ability to perform HoAcAcMS dosimetry would be highly desirable. Reliable MRI dosimetry has already been demonstrated in a clinical setting for liver radioembolisation using HoPLLAMs (22). Recently in an experimental setting, MRI dosimetry after intratumoral HoPLLAMs was demonstrated in a VX-2 tumour bearing animal with promising results (23). Implementing similar scan protocols for the final experimental set-up would be desirable. Note that correction for a higher holmium percentage per holmium sphere (18.7% vs 43% weight/weight ratio) should be taken into account.

Tumour growth was measured using anatomical T_2W TSE MRI images to evaluate tumour response to the treatment. During the measurements needed to calculate tumour volume, it sometimes proved difficult identifying the tumour borders needed to draw accurate region of interests. This was largely due to artefacts on anatomical T_2W TSE scans caused by HoAcAcMS. Indeed, the same paramagnetic properties of holmium and resulting signal voids used to visualise HoAcAcMS distorts the T_2W TSE anatomical MRI image intended for tumour depiction. Importantly, over- or underestimating tumour volume could be the result. Therefore the reliability of MRI to accurately measure tumour volume to assess tumour response should be thoroughly reviewed. Other options to assess tumour response using MRI include functional MRI such a Difusion Weight Imaging (DWI). As demonstrated by van de Maat et al. , the presence of holmium induces local field gradients causing signal reduction on DWI images and complicated apparent diffusion coefficient (ADC) characterization. This leads to decreased ADC values (24). Because HoAcAcMs have a considerable high holmium content (43%), utilizing DWI will most likely be difficult. Contrast-CT could be considered as an alternative for MRI to measure tumour volume post treatment. In CT imaging, the high attenuation properties of holmium result in white artefacts on CT. Since contrast fluid also result in whitening of the tumour tissue on CT images, differentiating between holmium and contrast agent indicating tumour tissue might be problematic. Pre contrast and post contrast CT imaging to assess attenuation changes could prove helpful to overcome this issue. This should first be tested ex-vivo before implementation. Although less precise, ultrasound could also be considered to measure the tumour dimensions (L,H,D) post treatment. Alternative options for functional imaging include dynamic computed tomography (DCE-CT). This technique has already been used for the evaluation of tumour vascularity and tumour response after radiation therapy in human head and neck cancer (25). DCE-CT uses the temporal changes in attenuation in the vascular bed and tissue during rapid CT acquisitions after i.v. administration of contrast agent. By doing so, the

vascular support in the tumour tissue can be assed using commercially available software (26). The high attenuation coefficient of holmium can have negative implications on these measurements. However, this has yet to be investigated. Another technique that deserves attention is Multi-Energy CT. It can be used to identify k-edges of elements within the diagnostic energy range instead of relying on the attenuation coefficient to differentiate heavy elements (27). Holmium, being an element with a high Z-value could very well be differentiated from other contrast agents with high Z-values like gadolinium using this technique. Also, CT based HoAcAcMS quantification and dosimetry could benefit from this technique because it can potentially improve the specificity for HoAcAcMS and therefore its accuracy and reliability.

Measurements of residual activity of all syringes and needles after treatment showed a retention of 22% (mean) of ^{166}HoAcAcMs. Presumably caused by premature settling of HoAcAcMs during treatment, also observed by Bult et al. (3, 6, 20). However, the calculated tumour absorbed dose was between 195.2 Gy and 273.6 and was close to the intended 200 Gy. Measurements of pre-treatment activity of all syringes reveal that the pre-calculated amount of MBq was exceeded in all dose preparations. Since there was no agreed pre-calculated correction for this known issue, initial overdosing could be due to the expertise and personal experience of the radiological technician. If all dose preparations are done by the same person (as in the present study), this doesn't have to be a problem because of presumable small personal variations. Preferably, a more consistent method should be used described in an experimental protocol in future experiments. For example, using a fixed agreed pre-calculated correction for the activity, based on the available literature and personal experience.

Table IV Imaging techniques and possible problems caused by HoAcAcMS

Image Technique	**Image modality**	**Purpose(s)**	**Technique based on**	**Possible problems caused by HoAcAcMS**
Anatomical T_2W TSE scan	MRI	-Tumour depiction -Tumour volume calculations	Highlights differences in T_2 relaxation time	Distortion of anatomical tumour architecture due to paramagnetic properties of holmium
Contrast CT	CT	-Tumour depiction -Tumour volume calculations	Changes in attenuation in the vascular bed and tissue	Differentiation between HoAcAcMS and contrast agent due to the high attenuation coefficient of holmium
Diffusion Weighted Scan	MRI	-Tumour depiction -Tumour volume -Tumour function	The degree of water mobility characterized by means of ADC	Signal reduction on DWI images caused by the paramagnetic properties of holmium
Dynamic CT	CT	- Tumour depiction - Tumour function	Temporal changes in attenuation in the vascular bed and tissue	Difficulty measuring accurate local attenuation changes due to the high attenuation coefficient of holmium
Multi Energy CT	CT	- Tumor depiction - Tumour volume - Quantification of HoAcAcMS? - HoAcAcMS dosimetry?	Identifying K-edges	-

In the final distribution and dose effect study, three dose cohorts are recognised (200 Gy, 400 Gy and 800 Gy). If the same tumour volumes were treated in the 800 Gy dose cohort, then the activity had to be increased fourfold. Both the amount of HoAcAcMS (mg) and neutron irradiation time of ^{165}HoAcAcMs can be increased to achieve a rise in activity. However, increasing the amount of HoAcAcMS (mg) could lead to incomparable results between dose cohorts regarding distribution. Therefore, the only variable that should be changed to allow a higher activity is the neutron irradiation time of the ^{165}HoAcAcMs. Since longer irradiation times could have an impact on the microsphere integrity, a maximum irradiation time should be determined (10). Logically, this is best done for the highest dose cohort (800 Gy) and for the largest allowable tumour volume. Once this is determined, the neutron irradiation time can be downscaled to preserve a relative same amount of HoAcAcMS (mg) between dose cohorts.

In conclusion, multimodality imaging for the purpose of investigating *in vivo* distribution of ^{166}HoAcAcMS after intratumoral injection is feasible. All modalities used have their own characteristics and performance issues that should be taken into account when designing the final experimental set-up (21). Combining multiple imaging modalities to complement each other can overcome individual limitations and give more useful and accurate results. For example, SPECT is known for its high intrinsic sensitivity and detectability for activated HoAcAcMS but has low temporal and spatial resolution. Thus making it very suitable for detection of possible HoAcAcMS shunting to organs after injection, but not for detailed distribution pattern analysis of HoAcAcMS inside (tumour)tissue. MRI or CT can complement SPECT for having far better spatial and temporal resolution. Although CT has an advantage over MRI for spatial resolution, the possible utilization of MRI based holmium microsphere dosimetry is an important advantage. Therefore being the better choice for the final experimental set-up. Theoretically, HoAcAcMS dosimetry using CT should also be possible using the high attenuation coefficient of HoAcAcMS and changes in tissue density before and after treatment. The feasibility of CT based HoPLLAMs dosimetry after intratumoral injection has recently been demonstrated with promising results (23). Since combined CT/SPECT is readily available at the UMCU, this combination would be more practical, rendering faster protocols and could give better spatial and temporal resolutions. In this respect, efforts to improve CT dosimetry would be worthwhile. In evaluating tumour response, *in vivo* MRI is suitable but image distortion of holmium must be taken into account (table IV). Therefore other options already mentioned should be thoroughly reviewed for best possible results in the final experimental set-up.

Acknowledgements

The author would like to thank dr. P.R. Seevinck for his MRI expertise and facilitation of the MRI experiments, Nikki de Wit for her assistance during the CT and SPECT experiments, Shireen Brewster MSc for her support and assistance with the experimental setup, animal experiments and histological coupes preparation and Dr. Ir. C. Oerlemans for his expertise and assistance during the animal experiments. Last, but surely not least the author would like to thank Remmert de Roos for his enthusiastic support, expertise and help during the HoAcAcMS preparation and radioactive experiments.

References

1. Seevinck PR. Multimodal imaging of holmium-loaded microspheres for internal radiation therapy [dissertation]. Utrecht, 9 November 2009; 2009.

2. Vente MAD. *Preclinical Studies on Holmium-166 (L-lactic Acid) Microspheres for Hepatic Arterial Radioembolization* [dissertation]. Utrecht, 9 July 2009.

3. Bult W, Vente MA, Vandermeulen E, Gielen I, Seevinck PR, Saunders J, et al. Microbrachytherapy using holmium-166 acetylacetonate microspheres: a pilot study in a spontaneous cancer animal model. Brachytherapy. 2013 Mar-Apr;12(2):171-7.

4. Steenbeek ID. Quantitative distribution assessment of HoAcAc microspheres and HoPLLA microspheres after direct injection. Graduate Thesis. Faculty of Veterinary Medicine, Utrecht University: 2011.

5. Veldwachter E. Experimental studies on interstitial microbrachytherapy with holmium-166 microspheres. Graduate Thesis. Faculty of Veterinary Medicine, Utrecht University: 2009.

6. Bult W, Kroeze SG, Elschot M, Seevinck PR, Beekman FJ, de Jong HW, et al. Intratumoral administration of holmium-166 acetylacetonate microspheres: antitumor efficacy and feasibility of multimodality imaging in renal cancer. PLoS One. 2013;8(1):e52178.

7. Hrycushko BA, Li S, Goins B, Otto RA, Bao A. Direct intratumoral infusion of liposome encapsulated rhenium radionuclides for cancer therapy: effects of nonuniform intratumoral dose distribution. Med Phys. 2011 Mar;38(3):1339-47.

8. van Es RJ, Franssen O, Dullens HF, Bernsen MR, Bosman F, Hennink WE, et al. The VX2 carcinoma in the rabbit auricle as an experimental model for intra-arterial embolization of head and neck squamous cell carcinoma with dextran microspheres. Lab Anim. 1999 Apr;33(2):175-84.

9. Tamargo RJ, Bok RA, Brem H. Angiogenesis inhibition by minocycline. Cancer Res. 1991 Jan 15;51(2):672-5.

10. Bult W, Seevinck PR, Krijger GC, Visser T, Kroon-Batenburg LM, Bakker CJ, et al. Microspheres with ultrahigh holmium content for radioablation of malignancies. Pharm Res. 2009 Jun;26(6):1371-8.

11. Vente MA, Nijsen JF, de Wit TC, Seppenwoolde JH, Krijger GC, Seevinck PR, et al. Clinical effects of transcatheter hepatic arterial embolization with holmium-166 poly(L-lactic acid) microspheres in healthy pigs. Eur J Nucl Med Mol Imaging. 2008 Jul;35(7):1259-71.

12. Brewster SS. Experimental studies on holmium therapy. Graduate Thesis. Faculty of Veterinary Medicine, Utrecht University: 2012.

13. Nakhgevany KB, Mobini J, Bassett JG, Miller E. Nonabsorbable radioactive material in the treatment of carcinomas by local injections. Cancer. 1988 Mar 1;61(5):931-40.

14. Ho S, Lau WY, Leung WT. Ultrasound guided internal radiotherapy using yttrium-90 glass microspheres for liver malignancies. J Nucl Med. 1997 Jul;38(7):1169-70.

15. Gao W, Liu L, Liu ZY, Wang Y, Jiang B, Liu XN. Intratumoral injection of 32P-chromic phosphate in the treatment of implanted pancreatic carcinoma. Cancer Biother Radiopharm. 2010 Apr;25(2):215-24.

16. Sjoholm H, Ljunggren K, Adeli R, Brun A, Ceberg C, Strand SE, et al. Necrosis of malignant gliomas after intratumoral injection of 201Tl in vivo in the rat. Anticancer Drugs. 1995 Feb;6(1):109-14.

17. Hafeli UO, Pauer GJ, Unnithan J, Prayson RA. Fibrin glue system for adjuvant brachytherapy of brain tumors with 188Re and 186Re-labeled microspheres. Eur J Pharm Biopharm. 2007 Mar;65(3):282-8.

18. Alic L, Haeck JC, Bol K, Klein S, van Tiel ST, Wielepolski PA, et al. Facilitating tumor functional assessment by spatially relating 3D tumor histology and in vivo MRI: image registration approach. PLoS One. 2011;6(8):e22835.

19. van Leeuwen BS, van Nimwegen SA, Zijlstra F, Oerlemans C, Kirpensteijn J, Nijsen JFW, et al. Feasibility of MR-guided needle-directed intratumoral HoMS delivery for localized radiation therapy in a large tumormodel. Poster Presentation. Joint Annual Meeting ISMRM-ESMRMB, Italy: 2014.

20. Bult W, de Leeuw H, Steinebach OM, van der Bom MJ, Wolterbeek HT, Heeren RM, et al. Radioactive holmium acetylacetonate microspheres for interstitial microbrachytherapy: an in vitro and in vivo stability study. Pharm Res. 2012 Mar;29(3):827-36.

21. Seevinck PR, Seppenwoolde JH, de Wit TC, Nijsen JF, Beekman FJ, van Het Schip AD, et al. Factors affecting the sensitivity and detection limits of MRI, CT, and SPECT for multimodal diagnostic and therapeutic agents. Anticancer Agents Med Chem. 2007 May;7(3):317-34.

22. van de Maat GH, Seevinck PR, Elschot M, Smits ML, de Leeuw H, van Het Schip AD, et al. MRI-based biodistribution assessment of holmium-166 poly(L-lactic acid) microspheres after radioembolisation. Eur Radiol. 2013 Mar;23(3):827-35.

23. Reijniers CB, van Leeuwen BS, Seevinck PR, van de maat GH, Nijsen JFW, Kirpenstijen J, et al. MRI-guidance of intratumoral injection of radioactive holmium microspheres in a Vx2 rabbit carcinoma: a model for microbrachytherapy of unresectable tumors. European Veterinary Conference Voorjaarsdagen. ; 2014.

24. van de Maat GH. Magnetic resonance imaging in 166Ho liver radioembolization [dissertation]. Utrecht University; 2013.

25. Hermans R, Meijerink M, Van den Bogaert W, Rijnders A, Weltens C, Lambin P. Tumor perfusion rate determined noninvasively by dynamic computed tomography predicts outcome in head-and-neck cancer after radiotherapy. Int J Radiat Oncol Biol Phys. 2003 Dec 1;57(5):1351-6.

26. Miles KA, Lee TY, Goh V, Klotz E, Cuenod C, Bisdas S, et al. Current status and guidelines for the assessment of tumour vascular support with dynamic contrast-enhanced computed tomography. Eur Radiol. 2012 Jul;22(7):1430-41.

27. Fornaro J, Leschka S, Hibbeln D, Butler A, Anderson N, Pache G, et al. Dual- and multi-energy CT: approach to functional imaging. Insights Imaging. 2011 Apr;2(2):149-59.